AsiaIntervention
2026;12:e115-e124
published online e-edition July 2026
DOI: 10.4244/AIJ-D-25-00091

ORIGINAL RESEARCH

Haemodynamic predictors of lesion progression in non-ischaemic tandem coronary stenoses

Marco Zuin[1,2,3], MD, MS; Alan Fong[4], MD, PhD; Giuseppe Marchese[3], MD; Andrea Bertolini[3], MD; Emanuele Rigatelli[5], MD; Marco Foroni[3], MD; Gianluca Rigatelli[3]*, MD, PhD

**Corresponding author: Department of Cardiology, Padova South Hospitals, Via Albere 30, 35043, Monselice, Padua, Italy. E-mail: gianluca.rigatelli@aulss6.veneto.it*

This paper also includes supplementary data published online at: https://AsiaIntervention.pcronline.com/doi/10.4244/AIJ-D-25-00091

ABSTRACT

BACKGROUND: Tandem coronary stenoses pose diagnostic challenges due to complex flow interactions that can obscure lesion severity when using traditional pressure-based indices such as fractional flow reserve (FFR). Computational fluid dynamics (CFD) can offer a detailed alternative haemodynamic assessment, but its prognostic value in non-haemodynamically significant tandem lesions remains unclear.

AIMS: We aimed to evaluate whether CFD-derived haemodynamic parameters could predict the 12-month progression of initially non-significant tandem lesions in the left anterior descending artery (LAD), defined by computed tomography (CT)-derived FFR (FFR-CT) ≥0.80.

METHODS: In a retrospective cohort of 60 1:1 propensity score-matched patients with tandem LAD stenoses, baseline and 12-month follow-up coronary CT angiography were performed. FFR-CT was computed using patient-specific CFD simulations, where FFR was defined as the ratio of the mean distal to aortic pressure under simulated hyperaemic flow conditions. CFD simulations quantified the time-averaged wall shear stress (TAWSS), oscillatory shear index (OSI), and relative residence time (RRT). Lesion progression was defined as diameter stenosis >70% and/or FFR-CT <0.80 at follow-up.

RESULTS: Baseline CT-derived FFR did not differ significantly between groups. Patients with lesion progression (n=30) exhibited significantly lower baseline TAWSS (0.32±0.10 Pa vs 0.82±0.20 Pa; p<0.001), higher OSI (0.22±0.06 vs 0.05±0.03; p<0.001), and prolonged RRT (1.9±0.6 s vs 0.7±0.3 s; p<0.001) compared with those with stable lesions. Multivariate analysis confirmed TAWSS, OSI, RRT, age, and diabetes as independent predictors of progression.

CONCLUSIONS: CFD-derived haemodynamic profiles strongly predict the 12-month progression of tandem LAD lesions despite a non-ischaemic baseline FFR-CT. The integration of CFD parameters with conventional physiology may improve the management of tandem coronary lesions beyond pressure-based indices alone.

KEYWORDS: CFD; coronary stenoses; disease progression; fractional flow reserve; tandem lesions

SUBMITTED ON 26/11/2025 - REVISION RECEIVED ON 12/03/2026 - ACCEPTED ON 27/03/2026

Tandem coronary stenoses, defined as two or more serial narrowing lesions within the same coronary artery, are observed in approximately 20-40% of patients undergoing coronary angiography for coronary artery disease.[1-3] When both lesions are obstructive, with a luminal diameter reduction >50%, their coexistence adds substantial complexity to the physiological assessment of coronary flow. Indeed, the haemodynamic interaction between proximal and distal stenoses can markedly influence pressure gradients and flow distribution, complicate the accurate assessment of each lesion's functional significance, and ultimately affect treatment strategy.[4,5]

Traditional physiology-based diagnostic techniques, such as fractional flow reserve (FFR)[6] and instantaneous wave-free ratio (iFR),[7] have well-recognised limitations in the setting of tandem or serial lesions. These methods rely on simplified assumptions regarding resistance distribution along the vessel, which may not hold true when multiple stenoses induce complex flow interactions. Specifically, the haemodynamic severity of each lesion is often underestimated in serial configurations,[8] as downstream resistance from additional stenoses can mask the true functional impact of a proximal lesion.[9] This complexity is further amplified by turbulent flow patterns, lesion eccentricity, and short interlesion distances, all of which contribute to non-linear pressure-flow relationships. Supporting this, studies such as the EMERALD II trial[10] have demonstrated the prognostic value of coronary computed tomography angiography (CCTA)-derived plaque characteristics and computational fluid dynamics (CFD) indices in predicting adverse cardiovascular outcomes.[11] In serial stenoses, proximal and distal lesions interact in a non-linear fashion, creating complex flow disturbances, pressure gradients, and recirculation zones that are not accurately captured by conventional pressure-based indices like FFR or iFR. As a result, even lesions deemed non-ischaemic by standard physiological assessment may exist within highly atherogenic local flow environments.

CFD offers a powerful, non-invasive, alternative approach to characterise local haemodynamic forces, such as wall shear stress and flow separation, providing insights into the rheological environment that drives atherosclerosis progression.[12,13] Recent advances in CFD modelling based on CCTA allow the assessment of parameters including time-averaged wall shear stress (TAWSS), oscillatory shear index (OSI), and relative residence time (RRT), all of which have been linked to endothelial dysfunction and plaque evolution.[14] Despite the growing application of CFD in coronary lesion assessment, the prognostic relevance of these haemodynamic metrics in patients with non-haemodynamically significant tandem lesions remains poorly understood. In particular, it is unclear whether adverse rheological conditions may predispose such lesions to progression, even when conventional physiological measures like FFR indicate functional insignificance at baseline.

Impact on daily practice

Computational fluid dynamic-derived haemodynamic parameters identify tandem coronary lesions that are at high risk of progression, even when computed tomography-derived fractional flow reserve is non-ischaemic. By enhancing personalised evaluation, this hybrid approach could contribute to determining the best interventional approach, enabling a shift from purely pressure-based decision-making to a comprehensive, rheology-informed strategy for complex tandem lesions.

This study evaluated whether CFD-derived haemodynamic parameters can predict the 12-month progression of initially non-significant tandem lesions in the left anterior descending artery (LAD) that are identified on CCTA. Patient-specific CFD modelling was used to uncover lesion-level rheological factors driving progression, complementing anatomical assessment. By integrating anatomical, physiological, and rheological data, this approach enables the early identification of high-risk lesions, allowing for personalised surveillance, tailored therapy, or selective intervention, thereby addressing the limitations of prior studies that focused on single lesions or conventional pressure-based indices[15].

Methods

STUDY POPULATION

Between 1 January 2023 and 1 September 2025, consecutive patients undergoing CCTA for any clinical indication at our institution were retrospectively screened. Inclusion criteria for the present study were (i) the presence of tandem coronary lesions involving the LAD, defined as two serial stenoses within the same vessel segment **(Figure 1)**; (ii) the presence of baseline lesions considered non-haemodynamically significant (computed tomography [CT]-derived FFR [FFR-CT] ≥0.80); and (iii) the availability of repeat CCTA and FFR-CT at 12-month follow-up, performed due to recurrent or new-onset ischaemic symptoms. Exclusion criteria included (i) tandem lesions involving the coronary ostium, (ii) significant concomitant stenoses in other major coronary arteries, (iii) prior coronary stenting or bypass surgery, (iv) advanced chronic kidney disease (estimated glomerular filtration rate [eGFR] <30 mL/min/1.73 m^2), (v) non-diagnostic image quality, (vi) incomplete clinical or imaging data, and (vii) pregnancy or breastfeeding. Applying these criteria, 98 eligible patients were initially identified. Of these, 21 were excluded for not meeting the inclusion criteria, leaving 77 patients. To minimise selection bias, 1:1 propensity score matching (PSM) was performed based on baseline demographic and angiographic characteristics, yielding a final study cohort of 60 patients: 30 with significant lesion progression at 12 months and 30 without progression **(Figure 2)**. Progression was defined as an increase in lesion severity leading to >70%

Abbreviations

CFD	computational fluid dynamics	**OSI**	oscillatory shear index	**TAWSS**	time-averaged wall shear stress
FFR	fractional flow reserve	**RRT**	relative residence time		

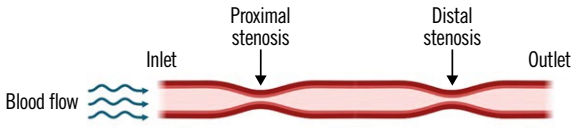

Figure 1. *Schematic representation of a coronary artery with tandem stenoses. The schematic illustrates blood flow entering the coronary artery at the inlet and passing through two distinct stenotic segments – a proximal stenosis and a distal stenosis – before exiting the outlet.*

diameter stenosis (DS) and/or FFR-CT <0.80 at follow-up CCTA.

Clinical variables – including age, sex, body mass index (BMI), hypertension, diabetes mellitus, smoking status, lipid profile, and medication use – were extracted from medical records. Low-density lipoprotein (LDL) cholesterol was calculated using the Friedewald formula. The study was approved by the local ethics board and was conducted in accordance with the study protocol, the Declaration of Helsinki, Good Clinical Practice principles, the Human Research Act, the Human Research Ordinance, and other applicable local regulations.

IMAGE ACQUISITION AND ANATOMICAL MODELLING

CCTA was performed using a 256-slice multidetector CT scanner with electrocardiogram gating. Beta blockers were administered prior to image acquisition to achieve a target heart rate of <65 bpm, with the specific agent and dosage determined at the treating physician's discretion. Additionally, a single dose of sublingual nitroglycerine (400-800 µg) was administered. CT acquisition parameters were adapted to patient BMI: 80-100 kVp/550 mA for BMI <25 kg/m^2 (high-definition mode), 100 kVp/550 mA for BMI 25-30 kg/m^2, and 120 kVp/600 mA for BMI >30 kg/m^2 (standard-definition mode). Iodinated contrast (80 mL) was used for all acquisitions. Non-contrast CT scans were acquired immediately prior to CCTA for coronary calcium scoring. Images were reconstructed with 3 mm slice thickness and analysed using semiautomated software (OsiriX [OsiriX Foundation]). Calcified lesions were defined as regions ≥130 Hounsfield units with an area ≥1 mm^2. The Agatston score was calculated for each patient by summing the weighted scores across all the coronary segments, following standard methodology.

A lesion was considered significant if the lumen area stenosis exceeded 50%. The CFD-based FFR-CT was computed offline by blinded investigators and defined as the ratio of the mean distal coronary pressure to the mean aortic pressure under

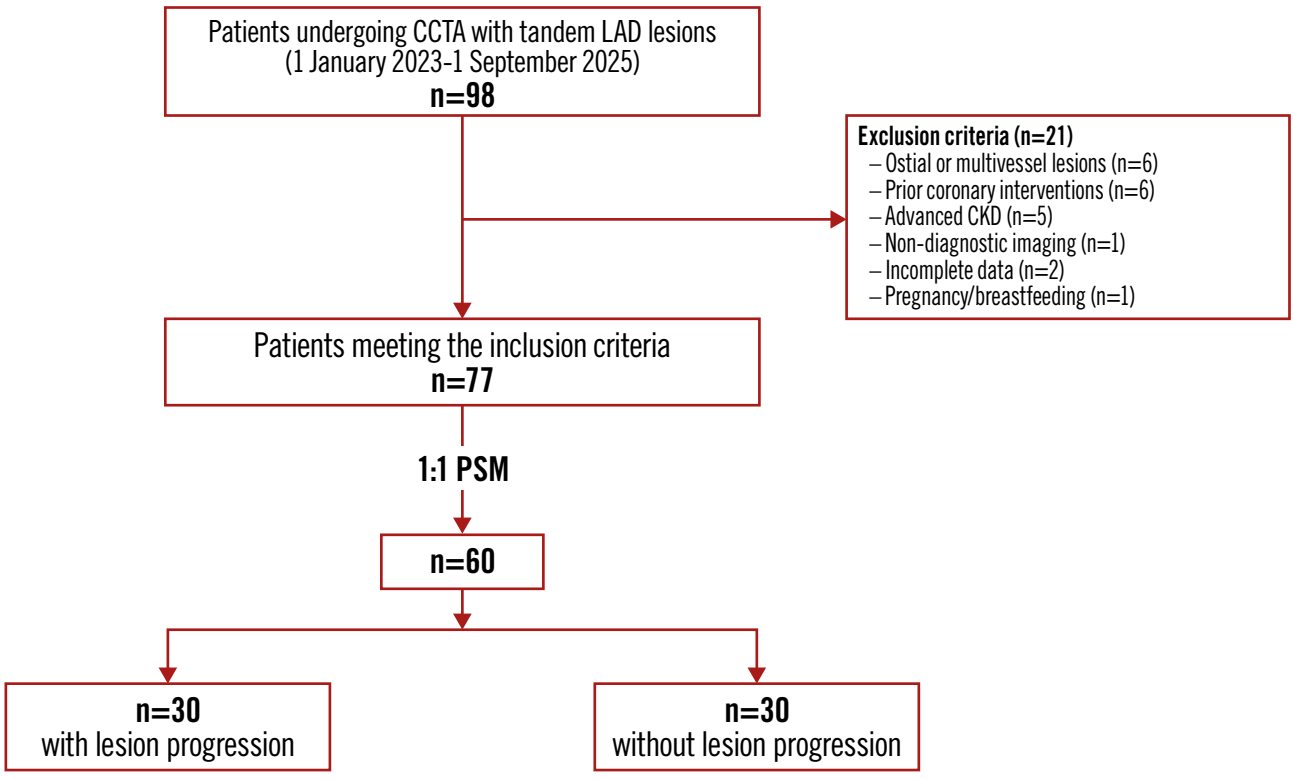

Figure 2. *Patient flow diagram. Flow of patients included in the study. A total of 98 consecutive patients undergoing coronary computed tomography angiography (CCTA) with tandem lesions of the left anterior descending artery (LAD) were screened between 1 January 2023 and 1 September 2025. After applying the inclusion and exclusion criteria, 77 patients were considered eligible. To reduce selection bias, 1:1 propensity score matching (PSM) was performed based on demographic and angiographic characteristics, resulting in a final study cohort of 60 patients: 30 patients with lesion progression at 12-month follow-up and 30 patients without progression. CKD: chronic kidney disease*

simulated hyperaemic conditions.[16,17] A haemodynamically significant lesion was defined as a lesion with an FFR-CT value of ≤0.80.

Patient-specific three-dimensional (3D) coronary geometries were reconstructed from Digital Imaging and Communications in Medicine images using OsiriX and further refined in Rhinoceros 4.0 (Robert McNeel & Associates). Segmentation included the full LAD and the two tandem lesions, including adjacent proximal and distal vessel segments. Geometries were meshed using Ansys ICEM CFD (ANSYS Inc.) with tetrahedral elements and prism layers at the vessel wall for boundary-layer resolution. Mesh independence was confirmed through convergence testing. The final meshes consisted of 300,000-400,000 elements. Local mesh refinement (0.1 mm) was applied in stenotic regions. Inlet boundary conditions were defined using patient-specific aortic pressure, obtained non-invasively using brachial cuff blood pressure measurements taken immediately prior to or during the CCTA scan, while outlet boundary conditions incorporated lumped-parameter models to account for downstream microvascular resistance. Simulated hyperaemia was applied by reducing the distal microvascular resistance, mimicking pharmacological vasodilation. The pressure gradients across each lesion were computed as the difference between the mean proximal and distal pressures along the stenotic segment. The CFD-based FFR-CT was then calculated as the ratio of the mean distal coronary pressure to the mean aortic pressure under hyperaemic flow conditions. For tandem lesions, pressure drops across individual stenoses were quantified separately, allowing for the assessment of the interaction between proximal and distal lesions on overall coronary haemodynamics.

To further characterise the haemodynamic interaction between the two serial LAD stenoses, an additional flow-field analysis was performed, focusing on

- the recovery zone length, defined as the downstream distance required for the pressure and velocity fields to restabilise after each stenosis;
- the distal-to-proximal pressure ratio (Pd/Pa) profiles at rest and during simulated hyperaemia;
- the influence of the interstenotic distance and degree of stenosis on pressure recovery and local shear patterns.

Using the CFD models previously described, streamwise pressure gradients and velocity vectors were extracted at 0.1 mm intervals along the centreline. The recovery zone was identified as the region beginning at the distal throat of each stenosis and ending where the derivative of the pressure ratio (d[Pd/Pa]/dx) approached zero, indicating haemodynamic re-equilibration. All calculations were performed by investigators blinded to clinical outcomes to avoid bias.

COMPUTATIONAL FLUID DYNAMICS SIMULATIONS

CFD simulations were performed using Ansys Fluent 2023 (ANSYS Inc.). Blood was modelled as an incompressible, non-Newtonian fluid using the Carreau viscosity model, with a density of 1,060 kg/m^3.[18] Vessel walls were assumed rigid with a no-slip boundary condition. A steady-state flow regime was applied to approximate mid-diastolic coronary perfusion. Patient-specific coronary flow rates were estimated from the stroke volume and heart rate, which were derived from echocardiography. Inlet velocity was prescribed at the left main coronary ostium, while outlet boundary conditions for the LAD and left circumflex artery were determined using Murray's law.[18,19] To account for turbulence in lesions with greater than 70% stenosis, the shear stress transport k-ω turbulence model was employed, with an inlet turbulence intensity of 5%. Simulations were considered converged when residuals fell below 1×10^{-5}. Each simulation spanned three cardiac cycles to ensure periodic steady-state conditions, and the final results were exported for post-processing and visualisation using Tecplot 360 EX (Tecplot, Inc.).

HAEMODYNAMIC PARAMETER QUANTIFICATION

Key haemodynamic parameters were extracted from the CFD simulations to characterise the local flow environment associated with each tandem lesion. TAWSS was calculated as the mean magnitude of shear stress exerted on the endothelium throughout the cardiac cycle.[20] OSI, which quantifies the temporal variability in shear direction, was used to assess the degree of disturbed or reversing flow.[21] RRT, representing the average duration that blood elements remain near the vessel wall, served as an indicator of flow stagnation and atheroprone conditions.[22] To provide a comprehensive assessment of lesion-associated haemodynamics, each parameter was computed across an extended vessel segment encompassing the stenotic region as well as adjacent proximal and distal segments. Segmental averages were subsequently used for statistical comparisons between patients with and without lesion progression at follow-up **(Supplementary Table 1)**. For CFD analysis, calcified regions were included in the segmented 3D geometries to preserve vessel morphology and local lumen geometry. Segment-level analyses were performed to evaluate whether coronary calcium burden influenced CFD-derived haemodynamic parameters (TAWSS, OSI, and RRT).

STATISTICAL ANALYSIS

Continuous variables are presented as mean±standard deviation or median with interquartile range (IQR), according to the data distribution as assessed by the Shapiro-Wilk test. Categorical variables are reported as counts and percentages. Between-group comparisons were performed using the Student's t-test or Mann-Whitney U test for continuous variables and the χ^2 test or Fisher's exact test for categorical variables, as appropriate. To minimise potential confounding and selection bias, 1:1 PSM was conducted using a nearest-neighbour algorithm with a calliper width of 0.1. Propensity scores were estimated via multivariate logistic regression including the following covariates: age, sex, hypertension, and diabetes, as well as lesion-specific geometric features, including the degree of coronary stenosis, lesion length, and interlesion distance.

Although PSM is traditionally applied to balance treatment groups in observational studies, we applied it here to create well-balanced groups for a natural outcome (lesion progression). This design-based approach allowed for direct comparisons of CFD-derived haemodynamic parameters between matched patients while reducing potential confounding from baseline anatomical and clinical heterogeneity. In this setting, PSM,

compared with alternative methods, such as multivariate regression or inverse probability weighting, was also able to adjust for baseline differences offering intuitive pairwise comparison and limiting model dependence, which is advantageous in a relatively small cohort. For each stenosis, we quantified post-stenotic recovery zones and computed shear-derived indices along the vessel centreline. Segment-level correlations between recovery-zone length and shear metrics were assessed with Pearson correlation coefficients (r). Moreover, we also evaluated segment-level correlations between the total coronary calcium burden (Agatston score) and CFD-derived haemodynamic parameters (TAWSS, OSI, RRT); these were assessed using Pearson correlation coefficients. Univariate logistic regression was used to identify predictors of lesion progression, and variables with $p<0.10$ in the univariate analysis were included in a multivariate logistic regression model. Results are reported as odds ratios (ORs) with 95% confidence intervals (CIs). A *post hoc* analysis of CFD-derived parameters was also performed in patients with single-lesion progression. A two-sided p-value<0.05 was considered statistically significant. All analyses were performed using R software (R Foundation for Statistical Computing).

Results

BASELINE CHARACTERISTICS

A total of 60 patients with baseline non-haemodynamically significant tandem coronary lesions on CCTA were included and followed for 12 months **(Figure 2)**. Patients were stratified into two groups according to the presence or absence of disease progression. The progression group included patients exhibiting an increase in lesion severity at follow-up CCTA, while the no-progression group included those with stable lesions.

As shown in **Table 1**, there were no significant differences in demographic or clinical characteristics between the progression and no-progression groups. Age, sex distribution, BMI, prevalence of hypertension and diabetes, smoking status, and lipid profiles were comparable. Likewise, baseline anatomical and functional lesion parameters – including minimal cross-sectional area, lesion length, interlesion distance, and degree of angiographic stenosis – did not differ significantly between groups. The median Agatston coronary calcium score in the study cohort was 112 (IQR 48-256), with no significant difference between patients with lesion progression and those without progression (progressors: 118 [IQR 50-260] vs non-progressors: 105 [IQR 45-250];

Table 1. General characteristics of the enrolled population.

	Disease progression (n=30)	No disease progression (n=30)	*p*-value
Age, years	65.2±7.8	64.9±8.1	0.84
Female	12 (40)	12 (40)	1.00
BMI, kg/m²	27.1±3.2	26.8±3.1	0.62
Hypertension	18 (60)	18 (60)	1.00
T2DM	6 (20)	6 (20)	1.00
Current smoker	6 (20)	6 (20)	1.00
Former smoker	9 (30)	9 (30)	1.00
Total cholesterol, mg/dL	181±25	181±25	1.00
HDL-C, mg/dL	45±8	45±8	1.00
Triglycerides, mg/dL	150±40	150±40	1.00
LDL-C, mg/dL	106±18	106±18	1.00
CCTA			
Calcium score, HU	118 (50-260)	105 (45-250)	0.62
Baseline angiography			
Minimal CSA, mm²	6.0±1.1	6.0±1.2	0.99
Proximal lesion length, mm	8.2±2.0	8.0±1.9	0.66
Distal lesion length, mm	10.1±2.7	9.9±2.6	0.72
Interstenotic distance, mm	12.4±3.5	12.1±3.3	0.72
Proximal stenosis, %	38±6	38±6	0.99
Distal stenosis, %	41±5	40±4	
FFR	0.86±0.03	0.86±0.03	0.95
12-month CCTA			
Proximal stenosis, %	72±8	40±7	<0.001
Distal stenosis, %	78±9	42±8	<0.001
CT-derived FFR	0.82±0.06	0.84±0.05	0.12

Data are n (%), mean±standard deviation, or median (interquartile range). BMI: body mass index; CCTA: coronary computed tomography angiography; CSA: cross-sectional area; CT: computed tomography; FFR: fractional flow reserve; HDL-C: high-density lipoprotein cholesterol; HU: Hounsfield unit; LDL-C: low-density lipoprotein cholesterol; T2DM: type 2 diabetes mellitus

p=0.62). Segment-level correlation analyses demonstrated that the total coronary calcium burden did not significantly affect CFD-derived parameters: TAWSS (r=–0.12; p=0.34), OSI (r=0.10; p=0.41), and RRT (r=0.08; p=0.48).

At 12 months, patients in the progression group exhibited a marked increase in lesion severity, with a significantly higher percentage diameter stenosis in both lesions (proximal lesion: 72±8% vs 40±7%; distal lesion: 78±9% vs 42±8%; p<0.001 for both). Despite this progression, follow-up CT-derived FFR values remained above ischaemic thresholds in both groups (mean FFR: progressors: 0.82±0.06 vs non-progressors: 0.84±0.05; p=0.12).

CFD PARAMETERS AND LESION PROGRESSION

CFD-derived haemodynamic parameters were strongly associated with disease progression **(Table 2)**. Patients with progressing lesions demonstrated a markedly lower TAWSS, a higher OSI, and an increased blood RRT in both stenoses. Specifically, the mean TAWSS in progressing lesions was reduced by more than 50% compared with stable lesions (proximal lesions: 0.32±0.10 Pa vs 0.82±0.20 Pa; p<0.001). Moreover, OSI and RRT were significantly elevated in progressing distal lesions (distal lesion OSI: 0.22±0.06 vs 0.05±0.03; p<0.001; RRT: 1.9±0.6 s vs 0.7±0.3 s; p<0.001) **(Figure 3, Supplementary Figure 1)**.

RECOVERY-ZONE DYNAMICS AND THE INFLUENCE OF STENOSIS GEOMETRY

Across the cohort, the post-stenotic recovery distance increased exponentially with percentage DS. The relationship was well described by an exponential function (recovery distance=0.45×e^[0.035×DS]; R^2=0.81). Recovery distances were approximately 3-4 mm for a 30% stenosis, 6-8 mm for a 40% stenosis, 10-12 mm for a 50% stenosis, and greater than 15 mm for a 60% stenosis. A threshold at approximately 40% DS was associated with a significant prolongation of the recovery distance (p<0.001), consistent with the inflection point of the canonical haemodynamic curve. Patients with lesion progression had substantially longer recovery zones after both stenoses than non-progressors (stenosis 1: 13.8±3.2 mm vs 8.6±2.4 mm; stenosis 2: 15.2±3.5 mm vs 9.3±2.8 mm; p<0.001 for both comparisons). The interaction index, quantifying the overlap between the two disturbed-flow fields, was also markedly higher in progressors (41±12% vs 17±9%; p<0.001). Pressure-recovery analyses corroborated these observations. At rest, pressure returned to baseline within a distance of 6-10 mm in non-progressors but remained depressed for over 15 mm in progressors. Hyperaemia prolonged recovery in both groups, yet between-group differences were preserved. The plateau phase of the pressure profile closely aligned with the region in which wall shear stress normalised and oscillatory shear diminished **(Figure 3, Figure 4)**. Segments characterised by a prolonged recovery distance demonstrated a lower TAWSS (r=–0.71; p<0.001), a higher oscillatory shear index (r=0.63; p<0.001), and a longer relative residence time (r=0.68; p<0.001), indicating a consistent endothelial milieu favouring atherogenic remodelling.

PREDICTORS OF DISEASE PROGRESSION

Univariate logistic regression analysis identified multiple significant predictors of lesion progression **(Table 3)**, including decreased TAWSS, increased OSI, and prolonged residence time; these were all strongly associated with higher odds of disease progression (all p<0.001). Among clinical variables, age (OR 1.06 per year; p=0.01) and diabetes (OR 1.10; p=0.002) were also significant predictors, whereas baseline FFR-CT and LDL cholesterol levels were not. In the multivariate logistic regression, TAWSS (OR 1.32 per 0.1 Pa decrease, 95% CI: 1.12-1.56; p=0.001), OSI (OR 1.48 per 0.05 unit increase, 95% CI: 1.15-1.90; p=0.002), relative residence time (OR 1.41 per 0.5 s increase, 95% CI: 1.12-1.77; p=0.003), age (OR 1.04 per 1 year increase; p=0.03), and diabetes (OR 1.08; p=0.03) remained independent predictors of progression.

SINGLE-LESION PROGRESSION

Among the 30 patients with lesion progression, 4 patients (13%) exhibited progression in only 1 of the 2 tandem lesions: 2 cases in the proximal lesion and 2 cases in the distal lesion. *Post hoc* analysis of CFD-derived parameters in these patients demonstrated that the progressing lesion consistently showed a lower TAWSS, a higher OSI, and a prolonged RRT compared with the non-progressing lesion in the same vessel **(Supplementary Table 2)**. In contrast, the non-progressing lesion exhibited relatively preserved haemodynamic conditions, despite being part of a tandem configuration.

Discussion

This study investigated the prognostic value of CFD-derived haemodynamic parameters for predicting the 12-month progression of non-haemodynamically significant coronary tandem lesions involving the LAD. Our main findings were as follows.

Table 2. CFD-derived haemodynamic parameters in patients with and without disease progression at 12-month follow-up.

	Disease progression		No disease progression	
Metric	Proximal stenosis	Distal stenosis	Proximal stenosis	Distal stenosis
TAWSS, Pa	0.32±0.10	0.28±0.12	0.82±0.20*	0.78±0.18**
OSI	0.18±0.05	0.22±0.06	0.04±0.02*	0.05±0.03**
RRT, s	1.6±0.5	1.9±0.6	0.6±0.2*	0.7±0.3**

Values are presented as mean±standard deviation. Haemodynamic metrics were calculated for each of the two tandem stenoses (stenosis 1=proximal; stenosis 2=distal) in patients with and without angiographic progression of disease. *p<0.001 for the comparison of stenosis 1 between the progression and no-progression groups. **p<0.001 for the comparison of stenosis 2 between the progression and no-progression groups. CFD: computational fluid dynamics; OSI: oscillatory shear index; RRT: relative residence time; TAWSS: time-averaged wall shear stress

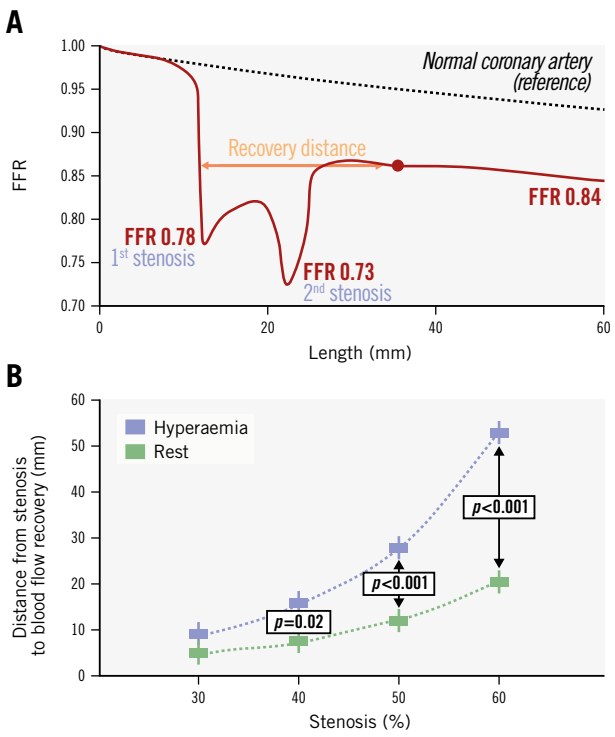

Figure 3. *Effect of the distance between two tandem stenoses. A) Distal-to-proximal pressure ratio profiles at rest (reference) and FFR profiles during hyperaemia for a first and second tandem stenosis of 38% and 41%, respectively. The values represent the mean stenosis severity in the analysed cohort. The red circle marks the distal location beyond which the FFR profile is no longer influenced by the presence of tandem stenoses. The dashed black line represents the FFR profile of an unobstructed artery under hyperaemic conditions. Immediately downstream of each stenosis lies a "recovery zone", characterised by a high-velocity jet region surrounded by recirculation zones associated with flow separation. The recovery zone is defined as the segment beginning at the distal stenosis and extending downstream until the streamwise derivative of the FFR signal returns to zero. B) The effect of stenosis severity on recovery distance. The extent of the recovery zone shows a similar exponential increase with increasing stenosis severity, reaching statistical significance at a stenosis of 40%. FFR: fractional flow reserve*

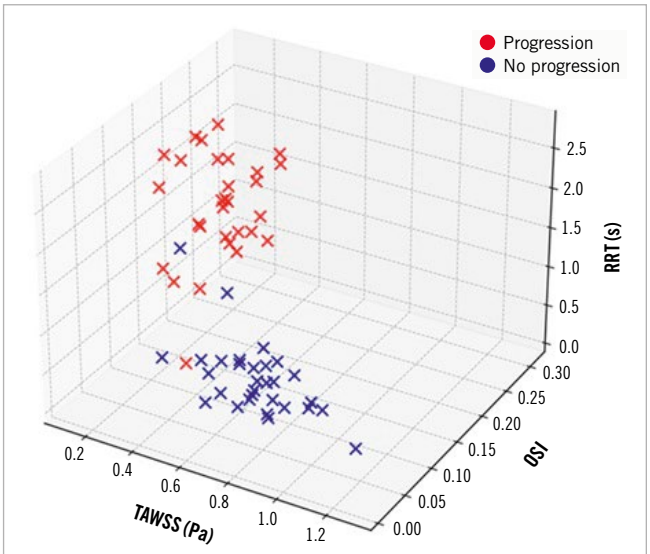

Figure 4. *Patient distribution according to TAWSS, OSI, and RRT. Three-dimensional scatterplot illustrating the distribution of patients based on key haemodynamic parameters derived from CFD: time-averaged wall shear stress (TAWSS; x-axis), oscillatory shear index (OSI; y-axis), and relative residence time (RRT; z-axis). The red crosses represent patients with lesion progression at 12 months, while the blue crosses indicate patients without progression. Patients with lesion progression are predominantly clustered in the region characterised by low TAWSS, high OSI, and prolonged RRT (lower left area and elevated along the RRT axis), highlighting the association between adverse haemodynamic profiles and lesion progression.*
CFD: computational fluid dynamics

- Adverse rheological conditions, specifically low TAWSS, elevated OSI, and prolonged RRT, were independently associated with significant lesion progression.
- These haemodynamic markers retained their predictive value even when the baseline CFD-based FFR-CT values were above the ischaemic threshold, suggesting that traditional physiology-based assessment alone may not capture future lesion behaviour.
- The interaction between proximal and distal stenoses created disturbed flow environments that likely promoted atherogenesis, a phenomenon not fully reflected by pressure-based indices.

These results highlight the complex relationship between local flow dynamics and atherogenesis in tandem coronary stenoses. While FFR remains the clinical standard for lesion-specific ischaemia assessment,[23] our findings suggest that its ability to predict subsequent disease progression, particularly in serial lesions, is limited. Despite comparable baseline FFR values between groups, patients with unfavourable shear stress profiles demonstrated significantly greater luminal narrowing at 12-month follow-up. This discordance underscores a potential shortcoming of current physiology-guided paradigms, as lesions deemed functionally insignificant may nonetheless be rheologically high risk.

The observation that the mean follow-up FFR-CT values remained above ischaemic thresholds even among progressing lesions supports the concept that FFR primarily reflects a system-level, pressure-derived metric, whereas local rheological forces act independently to drive plaque evolution.[24] Thus, a lesion may appear functionally benign according to FFR yet reside within a biomechanically adverse environment conducive to rapid progression. This distinction is particularly relevant for managing borderline lesions, where revascularisation decisions often hinge on physiological cutoffs.

The association between disturbed shear stress profiles and atherosclerotic progression is well established. Low

Table 3. Univariate and multivariate logistic regression analysis of predictors of disease progression.

	Univariate			Multivariate		
	OR	95% CI	*p*-value	OR	95% CI	*p*-value
TAWSS (per 0.1 Pa decrease)	1.50	1.32-1.70	<0.001	1.32	1.12-1.56	0.001
OSI (per 0.05 increase)	1.82	1.45-2.29	<0.001	1.48	1.15-1.90	0.002
RRT (per 0.5 s increase)	1.68	1.38-2.05	<0.001	1.41	1.12-1.77	0.003
Baseline FFR (per 0.01 decrease)	1.03	0.98-1.08	0.20	-		
Age (per 1 year increase)	1.06	1.02-1.13	0.01	1.04	1.01-1.09	0.03
Diabetes (yes vs no)	1.10	1.02-3.05	0.002	1.08	1.01-2.66	0.03
LDL (per 10 mg/dL increase)	1.05	0.92-1.20	0.45	-		

Continuous variables are expressed per the unit change indicated in parentheses. Variables with p<0.10 in the univariate analysis were included in the multivariate model. CI: confidence interval; FFR: fractional flow reserve; LDL: low-density lipoprotein; OR: odds ratio; OSI: oscillatory shear index; RRT: relative residence time; TAWSS: time-averaged wall shear stress

endothelial shear stress promotes endothelial dysfunction, leukocyte adhesion, and lipid deposition.[25] OSI, which reflects bidirectional or reversing flow, disrupts endothelial alignment and fosters a proinflammatory phenotype.[26] Similarly, prolonged RRT indicates regions of flow stagnation where atherogenic lipoproteins dwell near the vessel wall, enhancing subendothelial infiltration and foam-cell formation.[27]

In the context of tandem lesions, these adverse rheological effects are magnified. Interactions between proximal and distal stenoses create complex, non-linear pressure-flow relationships that promote turbulence and flow separation, especially when lesions are eccentric or closely spaced. Our results align with this pathophysiological model, showing that CFD-derived indices of disturbed flow were powerful predictors of lesion progression, independent of conventional clinical and angiographic parameters. These findings extend prior work by Park et al, who demonstrated strong diagnostic agreement between CFD and invasive FFR in tandem lesions.[28] Unlike that study, however, our investigation focuses on the prognostic value of CFD metrics, bridging an important gap in the literature.

A subset of patients showed progression in only one of the tandem lesions. In these cases, CFD analysis revealed that the lesion-specific haemodynamic environment, rather than the mere presence of a proximal or distal location, determined the risk of plaque progression. This finding underscores the lesion-level granularity offered by CFD, highlighting that even within serial stenoses, individual lesions can harbour distinct flow disturbances and atherogenic risk profiles. Such differentiation is not captured by traditional pressure-based indices like FFR, which reflect overall vessel-level physiology. These results reinforce the clinical value of integrating CFD-derived metrics into tandem lesion assessment, allowing the identification of high-risk lesions that may benefit from closer surveillance or early intervention, even when neighbouring stenoses remain stable.

Our study focused exclusively on tandem lesions of the LAD to ensure anatomical consistency and clinical relevance. The LAD supplies a large myocardial territory, and stenoses in this vessel are associated with a higher risk of adverse outcomes, making the early identification of high-risk lesions particularly important. While the haemodynamic interactions observed in the LAD may differ in other coronary arteries because of variations in vessel size, curvature, and branching patterns, the mechanistic insights regarding the impact of local flow disturbances on lesion progression are likely generalisable. Future studies including tandem lesions in the right coronary artery or circumflex artery are warranted to confirm the broader applicability of these findings and to explore vessel-specific haemodynamic effects.

In this study, we found that the post-stenotic recovery distance increased exponentially with stenosis severity, with a distinct inflection at approximately 40% diameter stenosis. This finding is consistent with classical fluid-dynamic models demonstrating that mild stenoses generate limited flow separation, whereas moderate stenoses trigger disproportionately larger recirculation zones and delayed re-establishment of laminar profiles. Earlier experimental work has shown that once a critical geometric threshold is exceeded, small increments in narrowing produce non-linear expansions of separated flow regions and induce oscillatory shear, a pattern reproduced in our patient-specific simulations.[29-31] The markedly prolonged recovery distances observed in progressors further support the central role of sustained flow disturbance in atherosclerotic remodelling. Prior studies using particle-tracking velocimetry and CFD have demonstrated that regions of extended recirculation or delayed reattachment promote endothelial dysfunction, inflammatory activation, and lipid accumulation.[32] The greater overlap between proximal and distal recovery zones in progressors suggests that tandem stenoses may behave synergistically, creating a compounded disturbance that exceeds the sum of the individual lesions, a phenomenon described in earlier analyses of serial stenosis haemodynamics.[33] Furthermore, pressure-recovery profiles provided physiological confirmation of these interactions. In agreement with prior observations that pressure equilibrates more rapidly than shear stress normalises, we found that pressure returned to baseline within a relatively short distance in non-progressors, whereas in progressors, pressure deficits persisted well into the distal vessel.[34] This dissociation highlights a known limitation of pressure-based indices: FFR, while robust for determining ischaemia, does not capture local flow separation, oscillatory shear, or prolonged residence time, mechanisms increasingly recognised as critical drivers of plaque progression and vulnerability.

In several cases, the substantial anatomical progression of tandem lesions (up to ~70% stenosis) was associated with

only minimal changes in CFD-based FFR-CT. This likely reflects the inherent limitations of CFD-based pressure simulations, including assumptions regarding microvascular resistance, steady-state flow, and rigid vessel walls, which may underestimate cumulative pressure drops in serial lesions. While this highlights the need for prospective validation against invasive FFR or commercial FFR-CT platforms, our study demonstrates that lesion-specific haemodynamic parameters (TAWSS, OSI, RRT) provide robust predictive information independent of absolute FFR-CT values.

Collectively, these results suggest that CFD analysis provides complementary information to traditional physiological assessment by identifying lesions that, while non-ischaemic at baseline, exhibit rheological signatures predictive of future progression. This insight could support more personalised management strategies, including closer surveillance, intensified medical therapy, or selective pre-emptive revascularisation. The absence of a predictive value for baseline FFR-CT underscores the inherent limitations of pressure-based indices in complex lesion morphologies. Tandem lesions violate the assumption of linear pressure-flow relationships on which FFR relies; distal lesions can mask the haemodynamic effect of proximal ones, leading to underestimation of disease severity.[8,35] By integrating vessel geometry and flow dynamics, CFD overcomes these limitations and offers a more comprehensive appraisal of lesion vulnerability.

To the best of our knowledge, this is the first study to demonstrate that CFD-derived haemodynamic parameters independently predict the progression of non-haemodynamically significant tandem coronary stenoses. By focusing on serial LAD lesions, we address a clinically relevant subset of coronary artery disease that is often underestimated by conventional physiological methods. Integrating patient-specific CFD modelling with longitudinal imaging provides a dynamic framework to examine how lesion geometry and local flow evolve over time, enhancing risk stratification beyond static anatomical or pressure-based measures. Importantly, our data show that lesions considered stable by FFR-CT may nonetheless harbour biomechanical conditions predisposing them to rapid progression.

Translating these findings into clinical practice will require standardised CFD workflows and validation in larger, multicentre cohorts. Collaboration among cardiologists, radiologists, computational scientists, and engineers will be crucial to ensure reproducibility, streamline analyses, and facilitate the timely integration of CFD into routine clinical decision-making.

Limitations

This study has several limitations. First, it is a retrospective, single-centre analysis with inclusion restricted to patients who underwent repeat CCTA due to recurrent or new-onset ischaemic symptoms. Consequently, the cohort is enriched for symptomatic individuals, which may introduce selection bias and limits the generalisability of our findings. Therefore, this work should be interpreted as an investigation of imaging and haemodynamic changes in a preselected symptomatic population, rather than a population-level prognostic study. Second, CFD simulations assume rigid vessel walls and simplified boundary conditions, which may not fully capture *in vivo* haemodynamics. Third, biological factors influencing plaque progression, such as systemic inflammation, medication adherence, or genetic predisposition, are not represented in the CFD models. Fourth, although RRT and other haemodynamic indices are promising markers of lesion vulnerability, their measurement remains technically variable and requires further standardisation. Additionally, we acknowledge that these lesion characteristics are mechanistically upstream determinants of CFD-derived haemodynamic parameters (TAWSS, OSI, RRT) and that matching based on these variables could potentially attenuate the observed associations ("overadjustment"). Nonetheless, we included them in the matching process to ensure the baseline comparability of lesion anatomy, thereby reducing confounding that could obscure the relationship between local flow disturbances and lesion progression. Segment-level analyses of CFD-derived metrics were performed independently of the matched anatomical variables to assess their mechanistic contribution to progression. Finally, the FFR-CT values in this study were derived from CFD simulations; validation with alternative computational platforms and comparison to invasive FFR are warranted to confirm robustness and reproducibility. Collectively, these limitations indicate that our results are hypothesis-generating, emphasising the need for prospective, multicentre studies in broader populations to establish clinically meaningful thresholds for adverse haemodynamic indices and support their integration into routine practice.

Conclusions

Advanced rheological parameters, including a low TAWSS, a high OSI, and a prolonged RRT, are strong, independent predictors of tandem lesion progression at 12 months, even in the absence of baseline ischaemia by CFD-derived FFR-CT. These findings highlight the potential of CFD to enhance risk stratification and personalise management in patients with tandem coronary stenoses. Incorporating CFD-based analysis into routine imaging workflows may represent a key step towards truly physiology-guided coronary care in this challenging lesion subset.

Authors' affiliations

1. Department of Translational Medicine, University of Ferrara, Ferrara, Italy; 2. Department of Cardio-Thoraco-Vascular Sciences and Public Health, University of Padova, Padua, Italy; 3. Department of Cardiology, Padova South Hospitals Schiavonia, Monselice, Italy; 4. Sarawak Heart Centre, Kota Samarahan, Malaysia; 5. University of Pavia, Pavia, Italy

Conflict of interest statement

The authors have no conflicts of interest to declare.

References

1. Freidoonimehr N, Atkins T, Marathe JA, Psaltis PJ, Arjomandi M. Evaluating the severity of tandem coronary stenoses: Insights from simulated FFR and iFR techniques. *J Biomech*. 2025;185:112707.

2. Appelman YE, Piek JJ, Redekop WK, et al. Clinical events following excimer laser angioplasty or balloon angioplasty for complex coronary lesions: subanalysis of a randomised trial. *Heart*. 1998;79:34-8.

3. Gaglione A, Hess OM, Buechi M, Pucillo A, Krayenbuehl HP. Coronary tandem lesions: effect of exercise. *Am Heart J*. 1992;123:1487-92.

4. Derimay F, Finet G, Rioufol G. Coronary artery stenosis prediction does not mean coronary artery stenosis obstruction. *Eur Heart J*. 2021;42:4401.

5. Scarsini R, Fezzi S, Leone AM, et al. Functional Patterns of Coronary Disease: Diffuse, Focal, and Serial Lesions. *JACC Cardiovasc Interv*. 2022;15:2174-91.

6. Renard BM, Cami E, Jiddou-Patros MR, et al. Optimizing the Technique for Invasive Fractional Flow Reserve to Assess Lesion-Specific Ischemia. *Circ Cardiovasc Interv*. 2019;12:e007939.

7. Sen S, Asrress KN, Nijjer S, et al. Diagnostic classification of the instantaneous wave-free ratio is equivalent to fractional flow reserve and is not improved with adenosine administration. Results of CLARIFY (Classification Accuracy of Pressure-Only Ratios Against Indices Using Flow Study). *J Am Coll Cardiol*. 2013;61:1409-20.

8. Modi BN, Rahman H, Ryan M, et al. Comparison of fractional flow reserve, instantaneous wave-free ratio and a novel technique for assessing coronary arteries with serial lesions. *EuroIntervention*. 2020;16:577-83.

9. Warisawa T, Howard JP, Kawase Y, et al. Difference in functional assessment of individual stenosis severity in serial coronary lesions between resting and hyperemic pressure-wire pullback: Insights from the GIFT registry. *Int J Cardiol*. 2020;312:10-5.

10. Koo BK, Yang S, Jung JW, et al. Artificial Intelligence-Enabled Quantitative Coronary Plaque and Hemodynamic Analysis for Predicting Acute Coronary Syndrome. *JACC Cardiovasc Imaging*. 2024;17:1062-76.

11. Li Kam Wa ME, Ezad SM, Modi B, et al. Randomized Comparison of Fractional Flow Reserve and Instantaneous Wave Free Ratio in Serial Disease. *JACC Cardiovasc Interv*. 2025;18:1617-27.

12. Zuin M, Rigatelli G, Vassilev D, Ronco F, Rigatelli A, Roncon L. Computational fluid dynamic-derived wall shear stress of non-significant left main bifurcation disease may predict acute vessel thrombosis at 3-year follow-up. *Heart Vessels*. 2020;35:297-306.

13. Bacigalupi E, Pizzicannella J, Rigatelli G, et al. Biomechanical factors and atherosclerosis localization: insights and clinical applications. *Front Cardiovasc Med*. 2024;11:1392702.

14. Ekmejian AA, Carpenter HJ, Ciofani JL, et al. Advances in the Computational Assessment of Disturbed Coronary Flow and Wall Shear Stress: A Contemporary Review. *J Am Heart Assoc*. 2024;13:e037129.

15. Vardhan M, Gounley J, Chen SJ, et al. Non-invasive characterization of complex coronary lesions. *Sci Rep*. 2021;11:8145.

16. Cai Z, Yu T, Yang Z, et al. Detecting lesion-specific ischemia in patients with coronary artery disease with computed tomography fractional flow reserve measured at different sites. BMC Med Imaging. 2023;23:76.

17. Alzhanov N, Ng EYK, Su X, Zhao Y. CFD Computation of Flow Fractional Reserve (FFR) in Coronary Artery Trees Using a Novel Physiologically Based Algorithm (PBA) Under 3D Steady and Pulsatile Flow Conditions. *Bioengineering*. (Basel) 2023;10:309.

18. Taylor DJ, Feher J, Halliday I, et al. Refining Our Understanding of the Flow Through Coronary Artery Branches; Revisiting Murray's Law in Human Epicardial Coronary Arteries. *Front Physiol*. 2022;13:871912.

19. Bennar W, Arroyo D, Oppé C, et al. Diagnostic Accuracy of Angiography-Derived Murray Law-Based Quantitative Flow Ratio (μQFR) Versus Pressure-Derived Fractional Flow Reserve (FFR) in Moderate to Severe Calcified Coronary Lesions-The DIAMOND Study. *Catheter Cardiovasc Interv*. 2025;106:377-83.

20. Mutlu O, Salman HE, Al-Thani H, El-Menyar A, Qidwai UA, Yalcin HC. How does hemodynamics affect rupture tissue mechanics in abdominal aortic aneurysm: Focus on wall shear stress derived parameters, time-averaged wall shear stress, oscillatory shear index, endothelial cell activation potential, and relative residence time. *Comput Biol Med*. 2023;154:106609.

21. Kok AM, Molony DS, Timmins LH, et al. The influence of multidirectional shear stress on plaque progression and composition changes in human coronary arteries. *EuroIntervention*. 2019;15:692-9.

22. Rigatelli G, Zuin M, Marchese G, et al. Residence time in complex left main bifurcation disease after stenting. *Cardiovasc Revasc Med*. 2024;61:1-5.

23. Wu J, Yang D, Zhang Y, et al. Non-invasive imaging innovation: FFR-CT combined with plaque characterization, safeguarding your cardiac health. *J Cardiovasc Comput Tomogr*. 2025;19:152-8.

24. De Bruyne B, Pijls NH, Heyndrickx GR, Hodeige D, Kirkeeide R, Gould KL. Pressure-derived fractional flow reserve to assess serial epicardial stenoses: theoretical basis and animal validation. *Circulation*. 2000;101:1840-7.

25. Zhou M, Yu Y, Chen R, et al. Wall shear stress and its role in atherosclerosis. *Front Cardiovasc Med*. 2023;10:1083547.

26. Ahmed ME, Leistner DM, Hakim D, et al. Endothelial Shear Stress Metrics Associate With Proinflammatory Pathways at the Culprit Site of Coronary Erosion. *JACC Basic Transl Sci*. 2024;9:1269-83.

27. Teng Z, Wang S, Tokgoz A, et al. Study on the association of wall shear stress and vessel structural stress with atherosclerosis: An experimental animal study. *Atherosclerosis*. 2021;320:38-46.

28. Park SJ, Ahn JM, Pijls NH, et al. Validation of functional state of coronary tandem lesions using computational flow dynamics. *Am J Cardiol*. 2012;110:1578-84.

29. Ku DN, Giddens DP, Zarins CK, Glagov S. Pulsatile flow and atherosclerosis in the human carotid bifurcation. Positive correlation between plaque location and low oscillating shear stress. *Arteriosclerosis*. 1985;5:293-302.

30. Friedman MH, Deters OJ, Mark FF, Bargeron CB, Hutchins GM. Arterial geometry affects hemodynamics. A potential risk factor for athersoclerosis. *Atherosclerosis*. 1983;46:225-31.

31. Kwak BR, Bäck M, Bochaton-Piallat ML, et al. Biomechanical factors in atherosclerosis: mechanisms and clinical implications. *Eur Heart J*. 2014;35:3013-20.

32. Chatzizisis YS, Coskun AU, Jonas M, Edelman ER, Feldman CL, Stone PH. Role of endothelial shear stress in the natural history of coronary atherosclerosis and vascular remodeling: molecular, cellular, and vascular behavior. *J Am Coll Cardiol*. 2007;49:2379-93.

33. Wang X, Shen Y, Shang M, Liu X, Munn LL. Endothelial mechanobiology in atherosclerosis. *Cardiovasc Res*. 2023;119:1656-75.

34. Banerjee RK, Ashtekar KD, Helmy TA, Effat MA, Back LH, Khoury SF. Hemodynamic diagnostics of epicardial coronary stenoses: in-vitro experimental and computational study. *Biomed Eng Online*. 2008;7:24.

35. Derimay F, Finet G, Rioufol G. Coronary artery stenosis prediction does not mean coronary artery stenosis obstruction. *Eur Heart J*. 2021;42:4401.

Supplementary data

Supplementary Table 1. Definitions and descriptions of the key haemodynamic parameters used in the cardiovascular flow analysis.

Supplementary Table 2. CFD parameters in patients with single-lesion progression.

Supplementary Figure 1. Patient-specific analysis of a computational fluid dynamics analysis of a 61-year-old male with tandem mild coronary stenoses.

The supplementary data are published online at: https://AsiaIntervention.pcronline.com/doi/10.4244/AIJ-D-25-00091

Supplementary data

Supplementary Table 1. Definitions and descriptions of the key haemodynamic parameters used in the cardiovascular flow analysis.

Hemodynamic Parameter	Definition	Formula
Time-averaged wall shear stress (TaWSS)	Refers to the time-averaged magnitude of wall shear stress (WSS) exerted by blood flow on the vessel wall during a cardiac cycle.	$TaWSS = \frac{1}{T}\int_0^T \lvert\vec{\tau}_\omega(t)\rvert dt$
Oscillatory shear index (OSI)	Refers to the degree of directional change in WSS during a cardiac cycle, , reflecting the oscillatory nature of blood flow	$OSI = \frac{1}{2}\left(1 - \frac{\lvert\int_0^T \vec{\tau}_\omega(t)dt\rvert}{\int_0^T \lvert\vec{\tau}_\omega(t)\rvert dt}\right)$
Relative residence time (RRT)	Combines the effects of WSS and OSI to quantify the time spent by blood particles near the vessel wall	$RRT = \frac{1}{TaWSS(1-2OSI)}$

Supplementary Table 2. CFD parameters in patients with single-lesion progression.

Patient ID	Lesion Location	Progression	TAWSS (Pa)	OSI	RRT (s)
6	Proximal	Yes	0.28	0.21	1.95
	Distal	No	0.76	0.04	0.72
9	Proximal	No	0.79	0.05	0.70
	Distal	Yes	0.31	0.23	1.88
18	Proximal	Yes	0.33	0.20	1.90
	Distal	No	0.81	0.05	0.68
21	Proximal	No	0.78	0.06	0.71
	Distal	Yes	0.30	0.22	1.92

Lesion progression was defined as an increase in diameter stenosis >70% and/or FFR-CT <0.80 at 12-month follow-up. OSI: Oscillatory shear index; RRT: Relative residence time; TAWSS: Time-averaged wall shear stress. In each patient, the progressing lesion consistently showed lower TAWSS, higher OSI, and prolonged RRT compared with the non-progressing lesion.

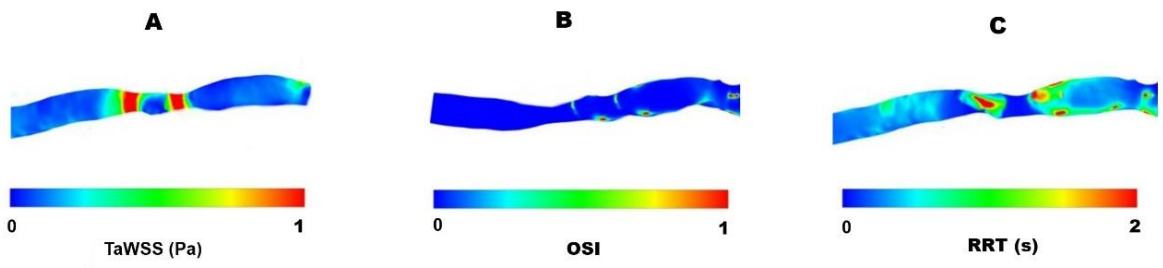

Supplementary Figure 1. Patient-specific analysis of a computational fluid dynamics analysis of a 61-year-old male with tandem mild coronary stenoses.

Panel A: Time averaged wall shear stress (TaWSS); Panel B: Oscillatory index (OSI); Panel C: Relative Resindent Time (RRT).